



Universiteit  
Leiden  
The Netherlands

## **Balanced epigenetic regulation of MHC class I expression in tumor cells by the histone ubiquitin modifiers BAP1 and PCGF1**

Wijdeven, R.H.; Luk, S.J.; Schoufour, T.A.W.; Zanden, S.Y.V.; Cabezuelo, M.; Heemskerk, M.H.M.; Neefjes, J.

### **Citation**

Wijdeven, R. H., Luk, S. J., Schoufour, T. A. W., Zanden, S. Y. V., Cabezuelo, M., Heemskerk, M. H. M., & Neefjes, J. (2024). Balanced epigenetic regulation of MHC class I expression in tumor cells by the histone ubiquitin modifiers BAP1 and PCGF1. *The Journal Of Immunology*, 212(3), 446-454. doi:10.4049/jimmunol.2300263

Version: Publisher's Version

License: [Licensed under Article 25fa Copyright Act/Law \(Amendment Taverne\)](#)

Downloaded from: <https://hdl.handle.net/1887/4094270>

**Note:** To cite this publication please use the final published version (if applicable).

# Balanced Epigenetic Regulation of MHC Class I Expression in Tumor Cells by the Histone Ubiquitin Modifiers BAP1 and PCGF1

Ruud H. Wijdeven,<sup>\*,†,‡</sup> Sietse J. Luk,<sup>§,1</sup> Tom A. W. Schoufour,<sup>\*,1</sup> Sabina Y. van der Zanden,<sup>\*</sup> Marta Cabezuelo,<sup>\*</sup> Mirjam H. M. Heemskerk,<sup>§</sup> and Jacques Neefjes<sup>\*</sup>

MHC class I (MHC-I) molecules are critical for CD8<sup>+</sup> T cell responses to viral infections and malignant cells, and tumors can downregulate MHC-I expression to promote immune evasion. In this study, using a genome-wide CRISPR screen on a human melanoma cell line, we identified the polycomb repressive complex 1 (PRC1) subunit PCGF1 and the deubiquitinating enzyme BAP1 as opposite regulators of MHC-I transcription. PCGF1 facilitates deposition of ubiquitin at H2AK119 at the MHC-I promoters to silence MHC-I, whereas BAP1 removes this modification to restore MHC-I expression. PCGF1 is widely expressed in tumors and its depletion increased MHC-I expression in multiple tumor lines, including MHC-I<sup>low</sup> tumors. In cells characterized by poor MHC-I expression, PRC1 and PRC2 act in parallel to impinge low transcription. However, PCGF1 depletion was sufficient to increase MHC-I expression and restore T cell-mediated killing of the tumor cells. Taken together, our data provide an additional layer of regulation of MHC-I expression in tumors: epigenetic silencing by PRC1 subunit PCGF1. *The Journal of Immunology*, 2024, 212: 446–454.

**M**ajor histocompatibility class I (MHC-I) molecules are critical initiators of the adaptive immune response against infected or malignant cells. These molecules, expressed on the surface of all nucleated cells, continuously present endogenous peptides to CD8<sup>+</sup> T cells, allowing specific detection of aberrant Ags and subsequent cytotoxic elimination of cells. In the MHC-I Ag presentation and processing (APP) pathway, intracellular proteins, including those of tumor, viral, and bacterial origin, are degraded by the proteasome, and the peptides that survive destruction by cytosolic peptidases are translocated into the endoplasmic reticulum by TAP1/TAP2, where they can be loaded onto MHC-I heterodimers consisting of HLA-I H chains with  $\beta_2$ -microglobulin (B2M). Peptide binding allows MHC-I molecules to be released from their endoplasmic reticulum chaperones and the peptide loading complex for transport to the plasma membrane, where antigenic peptides are displayed to CD8<sup>+</sup> T cells (1–3).

Given their importance in the recognition of intracellular pathogenic peptides, the expression of MHC-I is critically regulated, for example by IFNs. However, even though all nucleated cells express MHC-I, tissue expression varies widely, with low expression in, for example, brain cells and high expression in immune cells, especially dendritic cells (4, 5). In addition, MHC-I levels are modulated by pathogenic triggers. Viruses manipulate the APP pathway to downregulate MHC-I expression for their own survival (6). Also, tumor cells downregulate MHC-I expression to escape immune control or cancer immunotherapy (7–9). Modulation of MHC-I expression occurs at the transcriptional, epigenetic, as well as posttranscriptional level (9, 10). Recently, several genome-wide screens have

been performed to identify novel regulators of MHC-I expression on (tumor) cells originating from the hematopoietic lineage to understand differences in MHC-I expression (11–13). These screens confirmed the relevance of the known factors in the APP pathway for MHC-I expression, and, among others, identified the polycomb repressive complex 2 (PRC2) as a major epigenetic regulator of MHC-I expression (12–14).

Because checkpoint inhibitors that activate the immune system are especially successful in the treatment of melanoma, and MHC-I expression can be downregulated as a form of immune escape (8, 15–17), we aimed to identify factors in control of MHC-I expression in melanoma cells. Using a genome-wide CRISPR screen in Mel526 cells, we identified two epigenetic transcriptional regulators of MHC-I: BAP1 as a positive regulator and PCGF1 as a suppressor. PCGF1 and BAP1 act antagonistically in a wide range of tumor types, where PCGF1 facilitates deposition of ubiquitin at the H2AK119 site and BAP1 removes this histone modification. PCGF1 suppresses MHC-I expression in several MHC-I<sup>low</sup> tumor lines and mediates escape from T cell-mediated killing. This illustrates a broad role for PCGF1 and thus the polycomb repressive complex 1 (PRC1) complex in suppression of MHC-I expression.

## Materials and Methods

### *Cell culture, transfections, transductions, and Abs*

Mel526, Mel AKR, and HEK 293T cells were cultured in DMEM, K562 cells in RPMI 1640, and SK-N-BE, A673, and SK-ES1 cells in DMEM/F-12 (Life Technologies), all supplemented with 8% FCS. To generate viral particles for

\*Department of Cell and Chemical Biology, Oncode Institute, Leiden University Medical Center, Leiden, the Netherlands; <sup>†</sup>Department of Functional Genomics, Center for Neurogenomics and Cognitive Research, VU University Amsterdam, Amsterdam, the Netherlands; <sup>‡</sup>Alzheimer Center Amsterdam, Department of Neurology, Amsterdam UMC, Amsterdam, the Netherlands; and <sup>§</sup>Department of Hematology, Leiden University Medical Center, Leiden, the Netherlands

<sup>1</sup>These authors contributed equally to this work.

ORCID: 0000-0002-3390-7384 (R.H.W.); 0000-0002-6423-0994 (S.J.L.); 0000-0002-0475-2467 (T.A.W.S.); 0000-0001-5587-1514 (S.Y.v.d.Z.); 0009-0004-9144-8077 (M.C.); 0000-0001-6320-9133 (M.H.M.H.); 0000-0001-6763-2211 (J.N.).

Received for publication April 19, 2023. Accepted for publication November 13, 2023.

This work was supported by the Institute of Chemical Immunology, Nederlandse Organisatie voor Wetenschappelijk Onderzoek Gravitation Project ICI 0021 funded by

the Ministry of Education, Culture and Science of the government of the Netherlands, a Spinoza Premium, and by European Research Council Advanced Grant 694307 awarded to J.N.

Address correspondence and reprint requests to Prof. Dr. Jacques Neefjes, Department of Cell and Chemical Biology, ONCODE Institute, Leiden University Medical Center, Einthovenweg 2, 2333 ZC Leiden, the Netherlands. E-mail address: j.j.c.neefjes@lumc.nl

The online version of this article contains supplemental material.

Abbreviations used in this article: APP, Ag presentation and processing; B2M,  $\beta_2$ -microglobulin; gBAP1, gRNA BAP1; gCtrl, gRNA control; gPCGF1, gRNA PCGF1; gRNA, guide RNA; H2AK119ub, histone H2A in lysine 119; MHC-I, MHC class I; PRC1, polycomb repressive complex 1; PRC2, polycomb repressive complex 2.

Copyright © 2024 by The American Association of Immunologists, Inc. 0022-1767/24/\$37.50

the transductions, HEK 293T cells were transfected using polyethylenimine (Polysciences) with packaging plasmids pRSVrev, pHCMV-G VSV-G, and pMDLg/pRRE in combination with the lentiviral construct. Virus was harvested, filtered, and target cells were transduced in the presence of 8 µg/ml Polybrene (Millipore).

Abs used for flow cytometry were as follows: PE and FITC anti-human HLA-ABC (311405, BioLegend), PE anti-HLA-A2 (BB7.2, BD Biosciences), and allophycocyanin anti-HLA-BC (B1.23.2, Thermo Fisher Scientific). Abs for Western blot and chromatin immunoprecipitation (ChIP) experiments were as follows: mouse anti-BAP1 (sc-28383 [C-4], Santa Cruz), mouse anti-PCGF1 (sc-515371 [E-8], Santa Cruz), mouse anti-actin (A5441, Sigma-Aldrich), rabbit anti-H3K27me3 (07-449, Millipore), rabbit anti-histone H2A in lysine 119 (H2AK119ub) (8240, Cell Signaling Technology), rabbit anti-H3K4me3 (9751, Cell Signaling Technology), mouse anti-B2M (A16041A, BioLegend) TAP-1, TAP-2, HC-10, and HCA-2 (18, 19).

### CRISPR knockout screening

The human CRISPR Brunello genome-wide knockout library, containing four guide RNAs (gRNAs) per gene for a total of >19,000 genes, was a gift from David Root and John Doench (Addgene, no. 73178). After generating virus, 150 million Mel526 cells were infected at a multiplicity of infection of 0.3, and transduced cells were selected by puromycin (1 µg/ml). Six days after transduction, cells were stained for MHC-I and the 5% MHC<sup>low</sup>, but not negative, population was sorted. Cells were expanded and 1 wk later sorted again using the same gating settings. After this sort, cells were lysed, genomic DNA was isolated, and gDNAs were amplified using the established protocol (20). gRNAs were sequenced using the Illumina NovaSeq 6000 and inserts were mapped to the reference. gRNA enrichment compared with the unsorted cell population was performed using PinAPL-Py (21).

### Hit validation

For hit validation of the knockout screen, two individual guides per gene were cloned into the lentiCRISPR v2 vector (a gift from Feng Zhang, Addgene plasmid no. 52961) and cells were stably transduced with these guides or with the empty lentiCRISPR as a control. Cells were selected using puromycin, and pooled knockout cells were used for the analysis. Guide sequences were as follows: BAP1-1, 5'-CACGGACGTATCATCCACCA-3'; BAP1-2, 5'-TCTACCCATTGACCATTGGT-3'; PCGF1-1, 5'-CCACGAAGTAGCCGGCGCAT-3'; PCGF1-2, 5'-GCTCATATAGCGATAGTAG-3'; EED1, 5'-AA GAGAATGATCCATACCAC-3'.

### Flow cytometry

Cells were trypsinized and stained for the indicated Abs in 2% FCS/PBS for 30 min. After washing, cells were analyzed by the BD LSR II, and data were analyzed using FlowJo. For all experiments, mean fluorescence intensity was determined.

### cDNA synthesis and quantitative PCR

RNA isolation (Bioline) and cDNA synthesis (Roche) were performed according to the manufacturers' instructions. SYBR Green (Bioline) signal was detected on the Bio-Rad analyzer and normalized to GAPDH using the Pfaffl formula. Primers used for detection of signals were as follows: HLA-A forward, 5'-TGTGTTCTGTAGGCATA-3', reverse, 5'-TTGAGACAGAGATGGA GAC-3'; HLA-B forward, 5'-CTCCATCTCTGTCTCAACTT-3', reverse, 5'-CATCAACCTCTCATAGCA-3'; HLA-C forward 5'-GCTTCATCTCAG TGGGCTAC-3', reverse, 5'-CCTGGCGCTTGTACTTCTG-3'; B2M forward, 5'-GAGGCTATCCAGCGTACTCCA-3', reverse, 5'-CGGCAGGCATACTCATCTTTT-3'; TAP1 forward, 5'-TGCCCCGCATATTCTCCCT-3', reverse, 5'-CACCTGCGTTTTGCTCTTG-3'; TAP2 forward, 5'-GTTGGTGATGCT TTGTTCCA-3', reverse, 5'-AGTGCCTAGATGTGCAGTG-3'; GAPDH forward, 5'-TGTTGCCATCAATGACCCCTT-3', reverse, 5'-CTCCACGACGTACTCAGCG-3'.

### Western blotting

Cells were lysed directly in SDS sample buffer (2% SDS, 10% glycerol, 5% 2-ME, 60 mM Tris-HCl [pH 6.8], and 0.01% bromophenol blue). Samples were boiled before loading and proteins were separated by SDS-PAGE and transferred to Western blot filters. Blocking of the filter and Ab incubations were done in PBS supplemented with 0.1% (v/v) Tween 20 and 5% (w/v) milk powder. Blots were imaged using the Odyssey imaging system (LI-COR Biosciences) or Amersham Imager (uncropped Western blots can be found in Supplemental Fig. 3).

### ChIP-quantitative PCR

For ChIP, the DNA of 5 million cells per primer pair was crosslinked using 1% paraformaldehyde, quenched with glycine and washed with LB1, LB2

and LB3 as described in Schmidt et al. (22). Chromatin was fragmented using sonication and subjected to immunoprecipitation using the indicated Abs overnight. After extensive washing, DNA was reverse crosslinked, isolated, and amplified using the following primers covering the HLA-A and HLA-B promoter sites: HLA-A forward, 5'-TCCGCAGTTTCTTTTCTCCC-3', reverse, 5'-GGAGAATCTGAGTCCCGGTGG-3', HLA-B forward, 5'-TTGTGTAGGGAAACTGAGCAGC-3', reverse, 5'-TGTCTCA-CACCTCCATCCCAG-3'. Data were related to input signal to obtain relative DNA occupancy.

### T cell killing experiments

For generation of tumor-reactive T cells, T cell medium consisted of IMDM (Life Technologies, no. 21980-032) supplemented with 5% heat-inactivated FCS (Sigma-Aldrich, no. F7524), 5% human serum (Sanquin), 100 IU/ml IL-2 (Novartis), L-glutamine (Life Technologies, no. 25030-024), and penicillin/streptomycin (Life Technologies, no. 15141-122). Primary CD8<sup>+</sup> T cells were isolated from PBMCs using MACS beads (Miltenyi Biotec, no. 130-045-201) according to the manufacturer's instructions. CD8<sup>+</sup> T cells were subsequently stimulated with 0.8 µg/ml PHA and autologous total PBMCs as feeder cells, which were irradiated at 3500 rad. The ratio of CD8<sup>+</sup> T cells/feeder cells was 1:3. On day 2 after stimulation, CD8<sup>+</sup> T cells were retrovirally transduced with a clinically relevant TCR that recognizes the SLL peptide of PRAME that is presented in HLA-A 02:01 or HLA-B 07:02 (23, 24). As a negative control, T cells were transduced with a TCR that recognizes the NLV peptide of the pp65 protein from CMV (CMV TCR). In both TCR constructs, the constant domain was murinized for enrichment purposes. At day 7 after stimulation, TCR-transduced T cells were enriched using an allophycocyanin-labeled anti-murine TCR Ab (BD Biosciences, no. 553174) and anti-allophycocyanin beads (Miltenyi Biotec, no. 130-090-855) according to the manufacturers' instructions. Cell purity was >90% as measured by murine TCR expression. T cells were used in coculture assays on day 15 after stimulation. For coculture, SK-ES-1 cells were plated at a density of 30,000 cells in 50 ml of medium per well in a 96-well plate to form a near-confluent layer overnight. After visual confirmation of correct monolayers, 150 ml of T cell medium containing 5,000 or 15,000 T cells was added per well. A final concentration of 1 mM propidium iodide was added for quantification of cell death in live-cell imaging. Plates were imaged overnight using an Incucyte S3 (Sartorius) for phase contrast and red signal that detected death cells by propidium iodide. Incucyte software (Sartorius) was used for quantifying cell death in each well. For analysis of IFN-γ secretion by the TCR-transduced T cells, supernatants were harvested after overnight coculture and IFN-γ was measured using an ELISA kit (Diaclone, no. 851 560 020) according to the manufacturer's instructions. For analysis of CD137 expression on T cells, T cells were harvested after overnight coculture and stained using CD8-Pacific Blue (BD Biosciences, no. 558207) and CD137-allophycocyanin (BD Biosciences, no. 15816428). Cells were measured by an LSR II flow cytometer (BD Biosciences).

## Results

### Genome-wide screening identifies BAP1 and PCGF1 as opposite regulators of MHC-I expression

Given the importance of MHC-I in cancer immunotherapy, we searched for regulators of MHC-I expression in the context of melanoma, a major target of checkpoint inhibitor-based immunotherapy. To do so, we performed a genome-wide CRISPR knockout screen in HLA-A2<sup>+</sup> Mel526 melanoma cells, sorting for cells with low (but not negative) or high MHC-I expression after gene knockout (Fig. 1A). Cells were sorted twice and enrichment of genes was compared with the input. As expected, the peptide-loading complex genes TAP1, TAP2, and TAPBP were identified in the low MHC-I-expressing population, followed by deubiquitinating enzyme BAP1 (Fig. 1B, Supplemental Table I). In the high MHC-I-expressing population, PRC1 member PCGF1 was the main enriched gene. Interestingly, PRC1 drives polycomb gene repression by spreading ubiquitylation of H2AK119ub1, a mark that is removed by BAP1 (25–27). PRC1 consists of several subcomplexes, in which the PCGF subunits 1–6 demarcate locus specificity and function, whereas the catalytic subunits RNF1 (RING1A) and RNF2 (RING1B) catalyze H2AK119ub1 deposition (28, 29). Interestingly, several tumor types are characterized by loss of BAP1, while other tumors have increased PCGF1 activity (30–32).

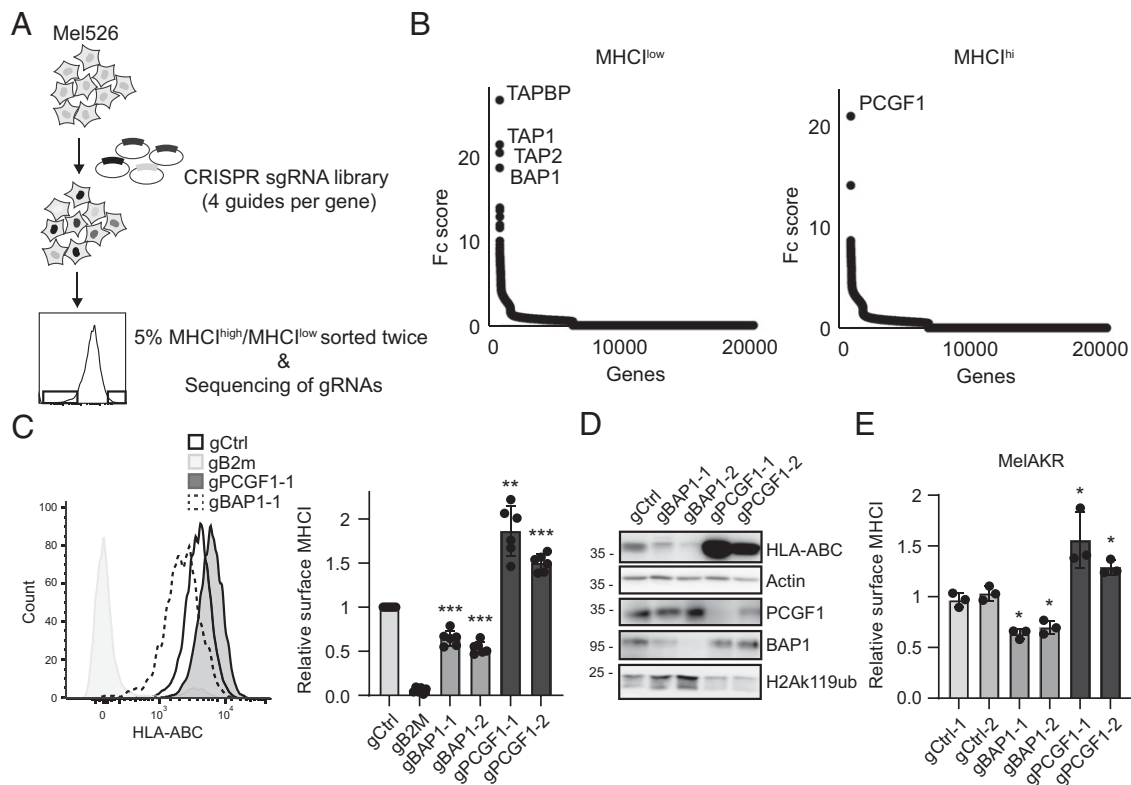


**FIGURE 1.** CRISPR screen identifies PCGF1 and BAP1 as opposite regulators of MHC-I expression in melanoma cells. **(A)** Schematic setup of the screen. Mel526 melanoma cells were transduced by a pooled CRISPR gRNA library and FACS sorted twice for cells displaying low (but not negative) or high MHC-I surface levels. **(B)** Fc scores for the different genes in the MHC-I<sup>low</sup> and MHC-I<sup>high</sup> populations as calculated using PinAPL-py. **(C)** Mel526 cells were transduced with the indicated gRNAs and pooled knockout clones were analyzed for surface MHC-I expression using flow cytometry. **(D)** Cells transduced as in **(C)** were lysed and expression of the indicated proteins were analyzed by SDS-PAGE and Western blot.  $\beta$ -Actin was probed as a loading control. **(E)** MelAKR cells were transduced with the indicated gRNAs and pooled clones were stained for surface MHC-I expression and analyzed by flow cytometry. For **(C)** and **(D)**, data represent three to six independent experiments ( $\pm$ SD). Statistical significance was determined by a paired Student *t* test. \**p* < 0.05, \*\**p* < 0.01, \*\*\**p* < 0.001.

To validate the results from the screen, BAP1 and PCGF1 were removed from Mel526 cells using two different gRNAs, and MHC-I surface levels were analyzed. Indeed, BAP1 removal decreased MHC-I expression by ~50%, whereas PCGF1 removal increased MHC-I surface levels (Fig. 1C). This was further confirmed by directly evaluating MHC-I expression by Western blot (Fig. 1D). To assess whether these hits were also operational in MHC-I expression control in other cells, another melanoma line, MelAKR, was transduced with the same gRNAs, yielding similar results (Fig. 1E). We thus identified the ubiquitin hydrolysis and ligase pair BAP1 and PCGF1 as positive and negative regulators of MHC-I expression, respectively.

#### PCGF1 controls MHC-I repression in multiple MHC-I<sup>low</sup> tumors

Several tumor types are known for their ability to strongly repress MHC-I expression, such as neuroblastoma and Ewing sarcoma (33, 34). This repression can be mediated by PRC2-dependent trimethylation of H3K27, and it contributes to immune escape (13). Recently, it has been shown that PRC1 and PRC2 activities can be linked, in combination silencing the expression of particular target genes (35–37). Because PCGF1 is a member of the PRC1 complex, this suggests that PCGF1 could also be involved in transcriptional repression of MHC-I in MHC-I<sup>low</sup> tumors. Indeed, genetic depletion of PCGF1 in K562 myelogenous leukemia cells (a model system often used to mimic MHC-I<sup>low</sup> tumor cells) robustly induced MHC-I expression (Fig. 2A, 2B). While these cells have very low MHC-I levels, BAP1 depletion still decreased the levels of MHC-I, suggesting that also in K562 cells the expression of MHC-I is dictated by the balance between the writing complex (PCGF1) and eraser (BAP1). When MHC-I was induced by exposure to IFN- $\gamma$ , the same balance

existed, indicating that PCGF1 and BAP1 also influenced IFN- $\gamma$ -mediated MHC-I levels (Fig. 2A). IFN- $\gamma$  did itself not affect BAP1 and PCGF1 expression, arguing for two independent modes of regulation (Fig. 2C, 2D).

To test the breadth of PCGF1-dependent regulation of MHC-I in MHC-I<sup>low</sup> tumors, we also tested neuroblastoma and Ewing sarcoma cell lines that are characterized by low MHC-I expression (33, 34). In all cell lines tested, depletion of PCGF1 robustly increased MHC-I expression (Fig. 2E), suggesting that PCGF1 is involved in the repression of MHC-I in various MHC-I<sup>low</sup> tumor cells.

#### General and HLA-B and HLA-C loci preferred regulation of MHC-I transcription by BAP1 and PCGF1

Epigenetic modifiers generally regulate transcription of genes, so we next tested whether BAP1 and PCGF1 affected expression of the different HLA loci. Depletion of BAP1 reduced expression of all three HLA locus products (HLA-A, HLA-B, and HLA-C) in both MHC-I<sup>normal</sup> and MHC-I<sup>low</sup> tumor cells, to an extent comparable to the surface levels (Fig. 3A, 3B). In contrast, depletion of PCGF1 increased transcription of HLA-B and HLA-C, whereas HLA-A levels were unaffected in MHC-I<sup>normal</sup> cells. In a MHC-I<sup>low</sup> cell line, SK-ES-1, an increase of HLA-A mRNA was detected by PCGF1 depletion, but this was considerably smaller compared with HLA-B and HLA-C. To further evaluate the HLA locus specific effects, Mel526 cells depleted for BAP1 and PCGF1 were stained with HLA-A2- and HLA-B/C-specific Abs and analyzed by flow cytometry. Whereas depletion of BAP1 decreased both surface HLA-A2 and HLA-B/C expression levels, PCGF1 depletion only increased HLA-B/C expression (Fig. 3C). This suggests that HLA-C

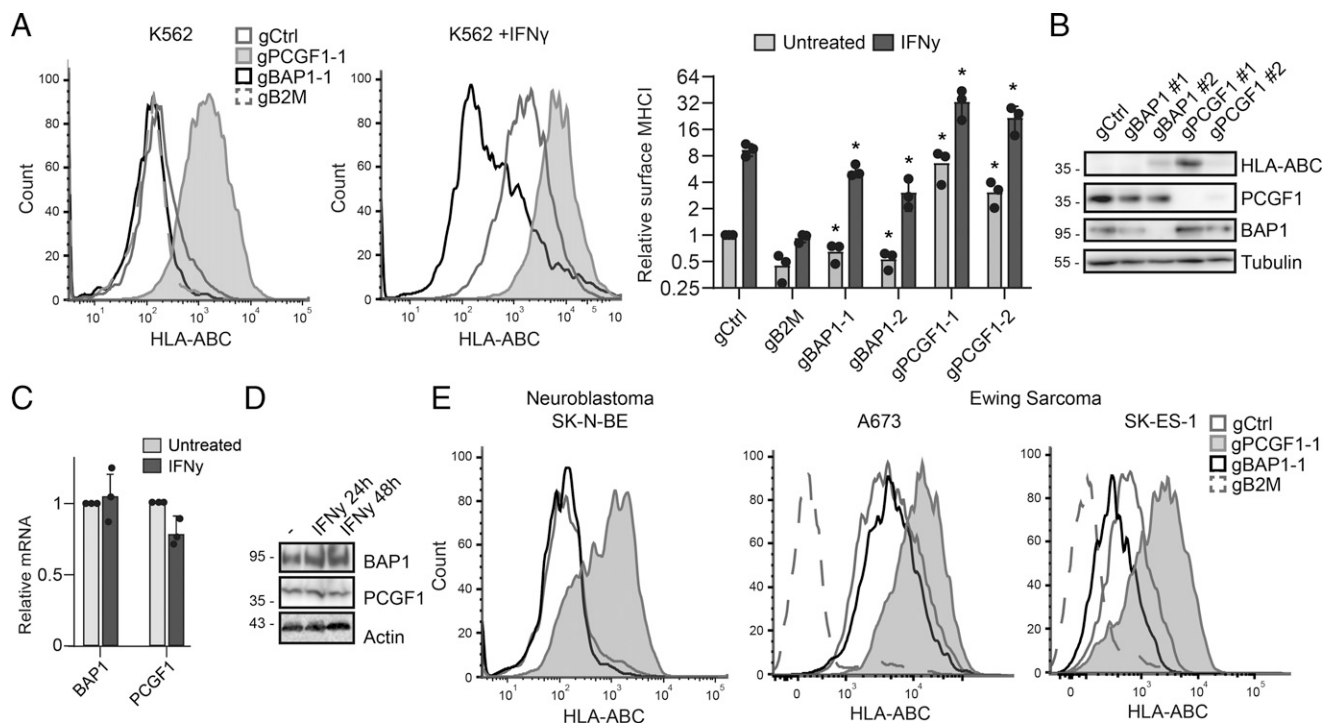


**FIGURE 2.** PCGF1 mediates suppression of MHC-I expression in MHC-I<sup>low</sup> tumor cells. **(A)** K562 cells were transduced with the indicated gRNAs and surface MHC-I expression on the pooled knockout cells were detected by flow cytometry. Cells were stimulated for 24 h with 100 ng/ml IFN- $\gamma$  when indicated; histograms are recorded with the same settings. Right, Quantification of surface MHC-I expression, relative to the untreated gCtrl cells, scaled as log<sub>2</sub>. Significance was determined by an ANOVA multiple comparison test (\* $p < 0.05$ ) and compared with the corresponding gCtrl sample. **(B)** K562 cells were lysed as in (A) and analyzed by SDS-PAGE and Western blot for the indicated proteins. **(C)** K562 cells were stimulated for 24 h with IFN- $\gamma$ , and expression of BAP1 and PCGF1 mRNA was analyzed using quantitative RT-PCR and normalized to GAPDH. **(D)** K562 cells were stimulated for the indicated time points with IFN- $\gamma$  and BAP1, and PCGF1 expression levels were determined using Western blot. **(E)** SK-N-BE neuroblastoma and A673 and SK-ES-1 Ewing sarcoma cells were transduced with the indicated gRNAs, and surface MHC-I expression on the pooled knockout cells was detected by flow cytometry. All data represent at least three independent experiments.

and especially HLA-B loci are under stricter control of PRC1 subunit PCGF1 than HLA-A. This regulation is reflected in the H2AK119ub levels at the promoter of these loci, because with ChIPs using H2AK119ub Abs the HLA-B promoter was consistently found to be modified more intensively than the HLA-A promoter (Fig. 3D). This modification was increased by depletion of BAP1, both at the HLA-A and HLA-B promoters, whereas depletion of PCGF1 decreased, but did not abrogate, H2AK119ub levels at HLA-B promoters (Fig. 3E). The remaining H2AK119ub modification at the promoter is possibly from one of the other PCGF subunits that can form a catalytic PRC1 complex. We then tested other histone modifications. Active histone mark H3K4me3 was not altered between the conditions, probably because the region is still heavily transcribed and almost all of the promoters were immunoprecipitated. However, PRC2-derived repressive mark H3K27me3 was significantly decreased after depletion of PCGF1 (Fig. 3F).

When other APP genes were tested for their control by PCGF1 modification of their promoters, a profile similar to HLA was found. TAP1 was very sensitive to loss of PCGF1, whereas the nearby gene TAP2 was affected to a more limited manner and B2M remained unchanged (Fig. 3G). Gene expression differences resulted in almost similar effects at the protein level, with the exception of B2M (Fig. 3H). B2M was slightly higher in the PCGF1 knockout and lower in the BAP1 knockout, probably because B2M that fails to associate to HLA molecules will be secreted as a free protein. Taken together, these data show that PCGF1 promotes H2AK119ub modifications to repress a selected number of APP genes, including HLA-B and HLA-C genes, whereas BAP1 functions more generally in the derepression of most of the APP genes.

#### PCGF1 and PRC2 in assembly repress MHC-I in MHC-I<sup>low</sup> tumors

Given the coupling between PCGF1/PRC1 and PRC2 and the reduction in H3K27me3 after PCGF1 depletion, we wondered whether PRC1 and PRC2 activities are linked, or whether they act independently from each other. To test the contribution of PRC2 to MHC-I suppression in our MHC-I<sup>normal</sup> and MHC-I<sup>low</sup> cells, Mel526 cells deficient for PRC2 core component EED were generated and phenotypically validated by their complete loss of H3K27me3 histone modifications (Fig. 4A). K562 cells, in line with other studies (13), strongly upregulated MHC-I following the loss of EED, but MHC-I expression on Mel526 cells was not affected by EED loss. Thus, PCGF1 apparently acted independently from PRC2 in Mel526 cells. Codepletion of EED and PCGF1 in K562 cells showed that the effect of the individual depletions is cumulative (Fig. 4B), again arguing for two separately regulated gene expression control pathways.

To further test this hypothesis, K562 cells were treated with the EZH2 inhibitor tazemetostat, which also abrogates H3K27me3 modifications by inhibiting the catalytic activity of EZH2. Under these conditions, MHC-I was upregulated more strongly than by genetic EED depletion, in line with previous results (13). Interestingly, the absence of PCGF1 in these cells hardly affected the levels of MHC-I (Fig. 4C), suggesting that when PRC2 is inhibited catalytically, PCGF1 is not functional anymore. This is in line with the concept that PRC1 and PRC2 act in assembly to impinge strong suppression of target genes. Taken together, our data suggest that in MHC-I<sup>normal</sup> cells, PCGF1 mediates H2AK119ub and facilitates mild suppression of MHC-I. However, when PRC2 is also active at the MHC-I promoter, this results in a higher suppression of MHC-I expression, yielding cells with a MHC-I<sup>low</sup> phenotype. In line with this notion

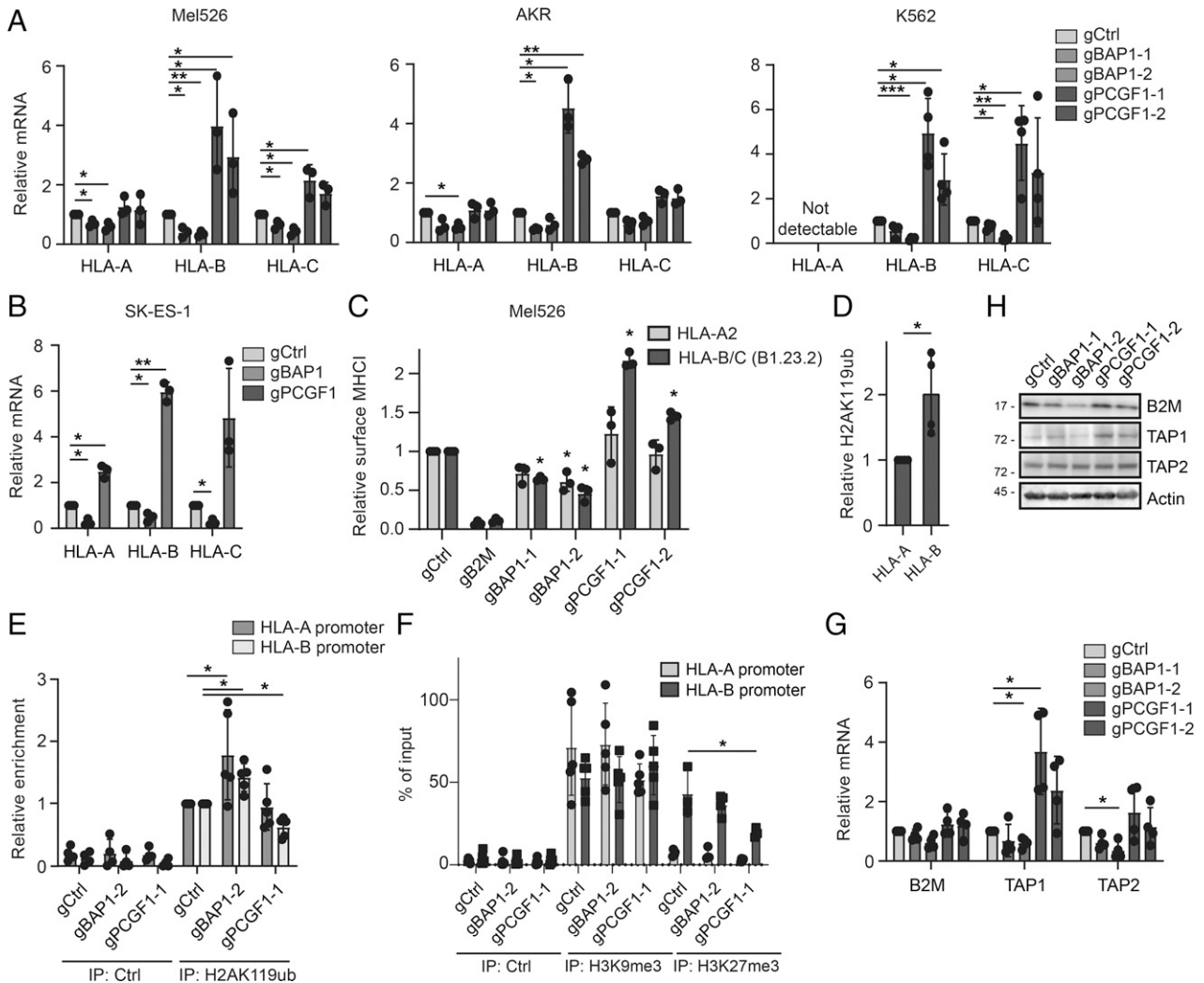


**FIGURE 3.** Locus-specific regulation of MHC-I transcription by PCGF1. **(A)** mRNA levels of the indicated genes were analyzed in Mel526, MelAKR, and K562 cells transduced with the indicated gRNAs by quantitative RT-PCR. Expression was normalized to GAPDH; HLA-A expression in K562 was too low to reliably detect. **(B)** SK-ES-1 cells transduced with the indicated gRNAs were used for mRNA expression analysis using quantitative RT-PCR. Expression was normalized to GAPDH. **(C)** Mel526 cells transduced with the indicated gRNAs were stained for surface HLA-A2 levels and HLA-B/C levels using allele- or locus-specific Abs and analyzed by flow cytometry. **(D)** H2AK119ub levels at the HLA-A and HLA-B promoters in Mel526 cells determined using ChIP experiments using an H2AK119ub Ab. Signal was detected using quantitative PCR (qPCR) and normalized to input levels and subsequently to the signal at the HLA-A promoter. **(E)** H2AK119ub-modified HLA-A and HLA-B promoters were isolated by ChIP from Mel526 cells transduced with the indicated gRNAs and quantified by qPCR. Signals were normalized to input DNA and divided by gCtrl signal levels. ChIP with an anti-GFP was used as control Ab. **(F)** ChIP-qPCR for H3K9me3 and H3K27me3 modification of the HLA-A and HLA-B promoter in cells depleted or not for BAP1 and PCGF1. Signals were normalized to input DNA and GFP Ab was used for the IP Ctrl. **(G)** mRNA level of the indicated genes were analyzed in Mel526 cells transduced with the indicated gRNAs using quantitative RT-PCR. Expression was normalized to GAPDH. **(H)** The cells as in **(G)** were analyzed for the expression of TAP1, TAP2, and B2M using Western blot. Actin was used as a loading control, and the molecular mass standards are indicated. All data represent means of at least three independent experiments ( $\pm$ SD). Statistical significance was determined by a paired Student *t* test. \**p* < 0.05, \*\**p* < 0.01, \*\*\**p* < 0.001.

that PCGF1 is essential but not sufficient for creating an MHC-I<sup>low</sup> phenotype, the expression levels of BAP1 and PCGF1 were comparable between MHC-I<sup>normal</sup> cells and the MHC-I<sup>low</sup> cells (Fig. 4D).

#### BAP1 and PCGF1 control T cell-mediated killing

Regulation of MHC-I expression by PCGF1 and BAP1 suggests that they influence evasion of CTL recognition and target cell killing. To test whether cells lacking PCGF1 or BAP1 have different sensitivities to CTLs, we used the SK-ES-1 cell line, which expresses HLA-A2 and the PRAME Ag. Whereas melanoma cells did not upregulate HLA-A2 after PCGF1 depletion, SK-ES-1 cells robustly increased HLA-A2 upon PCGF1 depletion, albeit not as much as total MHC-I levels (Figs. 3B, 5A). We subsequently exposed these SK-ES-1 cells to PRAME/A2-specific T cells and imaged the cells

in the presence of propidium Iodide to label dying cells (Fig. 5B). At both E:T ratios, gRNA PCGF1 (gPCGF1) cells were more sensitive to the T cells than gRNA control (gCtrl) cells, and the killing started much faster (Fig. 5C, 5D). gRNA BAP1 (gBAP1) cells, in contrast, were considerably less sensitive to T cell-mediated killing, in line with their decreased MHC-I levels. At the highest T cell concentration, all of the tumor cells in the gPCGF1 background were dead after 21 h, whereas the gCtrl cells still formed a viable monolayer and the gBAP1 cells were still mostly alive. When cells were first exposed to IFN- $\gamma$  to induce MHC-I expression, all of the target cells were rapidly killed (Fig. 5E), suggesting that above a certain threshold of MHC-I expression differences in CTL activity could not be detected. Because depletion of PCGF1 increased HLA-B and HLA-C expression even more, we repeated the assay with T cells

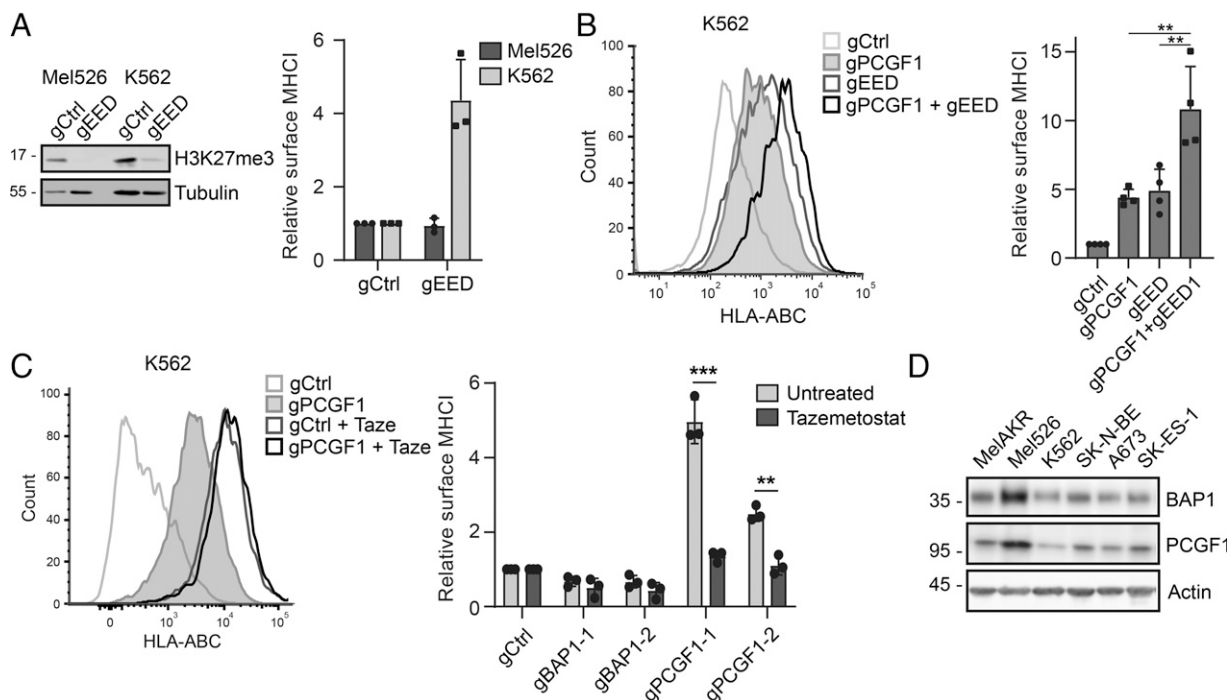


**FIGURE 4.** PCGF1, PRC1 and PRC2 suppresses MHC-I in MHC-I<sup>low</sup> tumors. (A) Mel526 and K562 cells were transduced with the indicated gRNAs, and the effects on MHC-I expression were determined by SDS-PAGE and Western blot (left) and flow cytometry (right). Surface MHC-I expression was normalized to the respective gCtrl cells. (B) K562 cells were depleted for PCGF1, EED, or both, and surface MHC-I expression was analyzed by flow cytometry. (C) K562 cells transduced with gCtrl, gBAP1, or gPCGF1 were treated with 2  $\mu$ M tazemetostat for 7 d and the effect on surface MHC-I expression was determined by flow cytometry. (D) Mel526 and the different MHC-I<sup>low</sup> cell lines were analyzed for BAP1 and PCGF1 expression using Western blot. Actin was used as a loading control, and the position of the molecular mass standards is indicated. Data represent three independent experiments ( $\pm$ SD). Statistical significance was determined by a paired Student *t* test. \*\**p* < 0.01, \*\*\**p* < 0.001.

recognizing PRAME presented by HLA-B7, another HLA allele expressed in SK-ES-1. Also in this study, PCGF1-depleted cells were sensitized to T cell-mediated killing (Fig. 5F). Between the gCtrl and gBAP1 cells no difference in killing was observed, probably because the tumor cells were able to overgrow the effect of the T cell killing, which was much less efficient due to the lower affinity of the TCR for its target.

The altered sensitivity to CTL-mediated target cell killing was accompanied by a corresponding alteration in T cell activation, because both the percentage of T cells expressing activation marker CD137 as well as the amount of IFN- $\gamma$  secreted by these T cells were higher in the PCGF1-depleted cells and lower in the BAP1-depleted cells (Fig. 5G, 5H). Thus, PCGF1-mediated suppression of MHC-I expression facilitates immune evasion, whereas BAP1-mediated silencing of MHC-I reduces immune recognition.

Next, we compared HLA-A/B/C expression levels in melanoma (skin cutaneous melanoma) to BAP1 and PCGF1 using The Cancer Genome Atlas database. No correlation between expression of these genes was observed (Supplemental Fig. 1A), likely because BAP1 and PCGF1 expression levels were significantly correlated (Supplemental Fig. 1B), a phenotype also observed in our cell lines (Fig. 4D). Furthermore, loss of BAP1 is known to increase M2 macrophage infiltration (38–40), observed in this study by an inverse correlation between BAP1 expression and HLA-DR $\alpha$  (MHC class II) (Supplemental Fig. 1C). MHC class II expression is highly correlated with MHC-I expression (Supplemental Fig. 1D), blurring a potential effect. However, expression of catalytic PRC1 subunit RNF2 did correlate inversely with HLA-A/B/C expression (Supplemental Fig. 1E), in contrast to other known transcriptional repressors of MHC-I (Supplemental Fig. 1F). Similar data were obtained in sarcoma (Supplemental Fig. 1G), where high expression of RNF2 strongly abrogated HLA-A/B/C expression. In line with this, high expression of RNF2 correlated with a poor

survival in both melanoma and sarcoma (Supplemental Fig. 2). High BAP1 levels in melanoma also associated with shorter survival rates, suggesting that BAP1 influences the tumor in multiple ways.

## Discussion

CD8<sup>+</sup> T cells recognize antigenic peptides in the context of MHC-I on tumor or pathogen-infected cells and thereby control disease. Consequently, tumor cells and pathogens have developed ways to interfere with expression of almost all components of the Ag presentation pathway, ultimately limiting MHC-I cell surface expression. In this study, we used genome-wide CRISPR knockout screening to identify an additional regulatory aspect of MHC-I expression and subsequent T cell-mediated killing: epigenetic silencing by PCGF1-mediated deposition of H2AK119ub, which is counteracted by BAP1.

Our data highlight an important role for PCGF1 in suppressing MHC-I expression at the transcriptional level, both in MHC-I<sup>normal</sup> and MHC-I<sup>low</sup> tumor cells. In several tumor lines derived from tumors known to have low MHC-I expression, such as neuroblastoma and Ewing sarcoma, depletion of PCGF1 increased MHC-I expression, even in cells where MHC-I was almost absent. However, the notion that PCGF1 depletion also increased MHC-I in MHC-I<sup>normal</sup> tumor cells suggests a more general role for PCGF1 in maintaining proper MHC-I levels. In line with this, a CRISPR screen in B cell lymphomas also identified PCGF1 as a regulator of MHC-I expression (12), and overexpression of PCGF1 is observed in multiple tumor types, including melanoma (31, 32). PCGF1 is part of the variant PRC1, which ligates ubiquitin onto histone H2AK119. We confirmed this H2AK119ub modification at the promoters of MHC-I. We tried to demonstrate that PCGF1 regulates MHC-I as part of PRC1, but depletion of the catalytic subunits RNF1 and RNF2 was lethal for the cells, as previously observed in other cells as well (41). Yet,

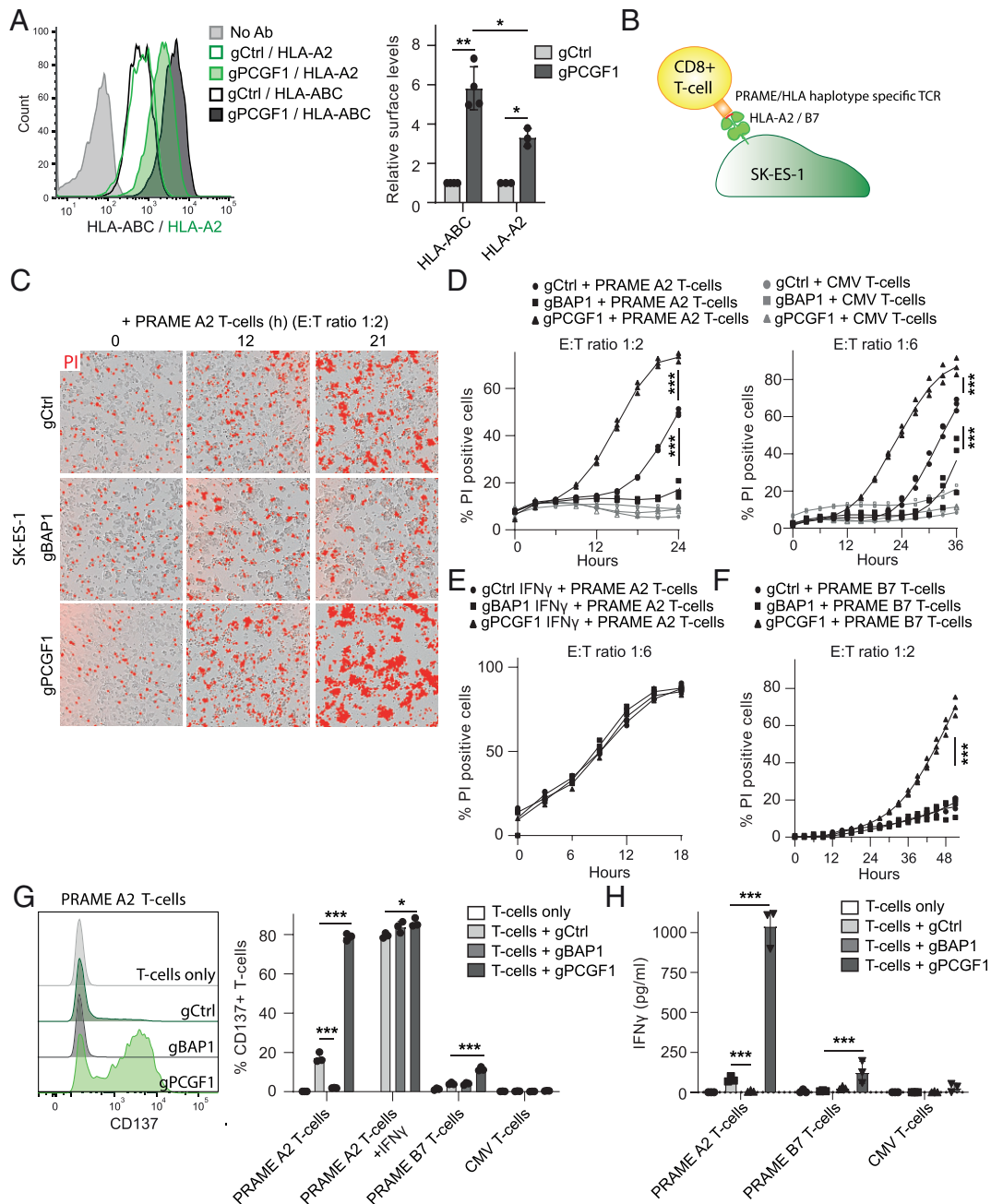


**FIGURE 5.** PCGF1 mediates escape from T cell-mediated cytotoxicity. **(A)** SK-ES-1 cells transduced with the indicated gRNAs were stained for surface HLA-A2 or surface HLA-ABC and analyzed by flow cytometry. Data represent mean  $\pm$  SD of three independent experiments. **(B)** Schematic setup of the T cell assays. SK-ES-1 cells are HLA-A2<sup>+</sup>, HLA-B7<sup>+</sup>, and PRAME<sup>+</sup> and are recognized by T cells transduced with an A2/PRAME- or B7/PRAME-specific TCR. **(C)** SK-ES-1 cells were seeded and 24 h later, A2/PRAME T cells were added at the indicated E:T ratio. Cells were imaged every 3 h using the Incucyte, and dead cells were detected by propidium iodide (PI) staining (original magnification  $\times 60$ ). **(D)** Quantification of T cell-mediated killing experiment from (C). The percentage of dead cells was quantified over three wells, with four images taken from every well, by dividing the PI-stained area by the cell-covered area. **(E)** Experiment as in (C), but SK-ES-1 cells were cultured with IFN- $\gamma$  for 24 h to induce MHC-I expression before addition of the T cells. **(F)** Experiment as in (C), but here B7/PRAME T cells were added to the SK-ES-1 cells and killing was monitored. **(G)** T cells exposed to the indicated SK-ES-1 cell lines were stained for CD137 surface marker expression 24 h after exposure to the indicated SK-ES-1 cells. Flow cytometry plot represents a merged image of the three analyzed wells, which are quantified on the right. **(H)** T cells were exposed to the indicated SK-ES-1 cells, and 24 h later supernatants were analyzed for the presence of IFN- $\gamma$  using ELISA. Data from (C)–(H) represent three technical replicates ( $\pm$ SD), and the experiments have been biologically replicated with similar results. \* $p < 0.05$ , \*\* $p < 0.01$ , \*\*\* $p < 0.001$ .

there are additional arguments why PCGF1 controls MHC-I expression as part of the PRC1 complex. First, the amount of H2AK119ub at the HLA-B promoter is reduced following PCGF1 depletion. Second, BAP1, which removes the ubiquitin deposited by PRC1 on H2AK119ub, has the opposite effect on MHC-I expression. Surprisingly, in several cell types HLA-C and especially HLA-B expression levels were

sensitive to PCGF1 depletion, whereas HLA-A remained unaffected or was upregulated to a lesser extent. In contrast, depletion of BAP1 decreased expression of all alleles, arguing that at least in some cell types PCGF1 has a preference for HLA-B and HLA-C, and HLA-A is only targeted when the balance is shifted toward higher PRC1 activity.

The polycomb repressor complexes PRC1 and PRC2 control the epigenome and their activities are linked. Ubiquitination of H2AK119 by PCGF1 facilitates PRC2 binding and subsequent local modification to H3K27me3 and gene silencing (37). However, they can also function as two independent pathways to facilitate gene silencing (42). Our data placing PRC1 in control of MHC-I expression are in line with findings that PRC2 suppresses MHC-I in MHC-I<sup>low</sup> tumors, and PRC2 depletion also affected primarily HLA-B and HLA-C expression (13). However, in MHC-I<sup>normal</sup> cells, PRC2 depletion had no effect on MHC-I expression, suggesting two modes of operation. In mode one only PCGF1-PRC1 is active, leading to mild suppression of MHC-I expression. In mode two, when PRC2 is also active, MHC-I is more strongly suppressed, resulting in MHC-I<sup>low</sup> tumors. Surprisingly, when PRC2 is inhibited chemically and not genetically, MHC-I is more strongly upregulated, and PCGF1-PRC1 depletion does not further increase MHC-I expression. This could arise from the inactive PRC2 occupying PCGF1-PRC1 binding sites, or because there are components of PRC1 used by the inactive PRC2 complex (43). Taken together, our observations in combination with previous findings support the model where PCGF1-PRC1 inflicts mild MHC-I suppression, whereas PCGF1-PRC1 in combination with PRC2 results in strong reduction of MHC-I expression.

To counteract H2AK119ub modifications and corresponding epigenetic silencing, the deubiquitinase BAP1 functions as the eraser and catalyzes H2AK119 deubiquitination. In line with this model, BAP1 depletion was found to decrease MHC-I expression by enhancing H2AK119ub at the HLA-A and HLA-B promoters. BAP1 decreased MHC-I on MHC-I<sup>normal</sup> and MHC-I<sup>low</sup> cells, as well as IFN- $\gamma$ -induced MHC-I expression. Given that BAP1 is depleted in several tumors, most prominently in uveal melanoma and mesothelioma, we reintroduced BAP1 in some of these cell lines to upregulate MHC-I. In two out of four lines (one uveal melanoma and one mesothelioma) MHC-I expression was indeed increased, but not in the other lines. This could be because cells often rewire their epigenetic landscape to accommodate BAP1 loss, or because in some cells PCGF1 might not be active (44, 45). The definitive impact of BAP1 on tumor progression is mixed, and highly context- and tumor-dependent, given its role in the repression of apoptotic factors (46) as well as immune infiltration (38–40). In a B16/F10 mouse melanoma model, deletion of BAP1 strongly reduced tumor growth (47), whereas in uveal melanoma reduced BAP1 levels are associated with shortened survival (48). Interestingly, the remaining B16/F10 mouse melanoma tumors in the BAP1 knockout situation expressed reduced H2-D1 transcript levels, although other APP genes were not (significantly) affected (47). Supporting an in vivo role for BAP1 in derepression of MHC-I genes, in a mouse trophoblast model expression of BAP1 strongly increased expression of H2-D1, H2-K1, TAP1, and TAP2 (49). Taken together, although a direct effect of BAP1 loss on tumor cells is reduced MHC-I expression, this effect might be negated or masked by an increased influx of immune cells.

Collectively, we identified and verified an additional layer of regulation of MHC-I expression: epigenetic silencing by H2AK119ub. Many tumor cells use this pathway to downregulate MHC-I expression, predominantly the HLA-B and HLA-C loci, and when combined with increased PRC2 activity, this leads to significant reduction of MHC-I expression and potential immune escape. Thus, targeting PCGF1 in the context of PRC1 would be an attractive mechanism to correct MHC-I expression and stimulate immune reactivity of tumor cells.

## Acknowledgments

We thank members of the Neeffjes group for valuable discussions and the Leiden University Medical Center Flow Cytometry Core Facility for help with cell sorting. We thank Anne Wouters for generating PRAME- and CMV-specific T cell lines.

## Disclosures

The authors have no financial conflicts of interest.

## References

- Pishesha, N., T. J. Harmand, and H. L. Ploegh. 2022. A guide to antigen processing and presentation. *Nat. Rev. Immunol.* 22: 751–764.
- Neeffjes, J., M. L. Jongsma, P. Paul, and O. Bakke. 2011. Towards a systems understanding of MHC class I and MHC class II antigen presentation. *Nat. Rev. Immunol.* 11: 823–836.
- Rock, K. L., E. Reits, and J. Neeffjes. 2016. Present yourself! By MHC class I and MHC class II molecules. *Trends Immunol.* 37: 724–737.
- Cebrián, C., V. D. Loike, and D. Sulzer. 2014. Neuronal MHC-I expression and its implications in synaptic function, axonal regeneration and Parkinson's and other brain diseases. *Front. Neuroanat.* 8: 114.
- Blum, J. S., P. A. Wearsch, and P. Cresswell. 2013. Pathways of antigen processing. *Annu. Rev. Immunol.* 31: 443–473.
- Arshad, N., M. Laurent-Rolle, W. S. Ahmed, J. C. Hsu, S. M. Mitchell, J. Pawlak, D. Sengupta, K. H. Biswas, and P. Cresswell. 2023. SARS-CoV-2 accessory proteins ORF7a and ORF3a use distinct mechanisms to down-regulate MHC-I surface expression. *Proc. Natl. Acad. Sci. USA* 120: e2208525120.
- Paulson, K. G., V. Voillet, M. S. McAfee, D. S. Hunter, F. D. Wagener, M. Perdicchio, W. J. Valente, S. J. Koelle, C. D. Church, N. Vandeven, et al. 2018. Acquired cancer resistance to combination immunotherapy from transcriptional loss of class I HLA. *Nat. Commun.* 9: 3868.
- Zaretsky, J. M., A. Garcia-Diaz, D. S. Shin, H. Escuin-Ordinas, W. Hugo, S. Hu-Lieskovan, D. Y. Torrejon, G. Abril-Rodriguez, S. Sandoval, L. Barthly, et al. 2016. Mutations associated with acquired resistance to PD-1 blockade in melanoma. *N. Engl. J. Med.* 375: 819–829.
- Taylor, B. C., and J. M. Balko. 2022. Mechanisms of MHC-I downregulation and role in immunotherapy response. *Front. Immunol.* 13: 844866.
- Dersh, D., J. Holly, and J. W. Yewdell. 2021. A few good peptides: MHC class I-based cancer immunosurveillance and immunoevasion. [Published erratum appears in 2020 *Nat. Rev. Immunol.* 20: 644.] *Nat. Rev. Immunol.* 21: 116–128.
- Jongsma, M. L. M., A. A. de Waard, M. Raaben, T. Zhang, B. Cabukusta, R. Platzer, V. A. Blomen, A. Xagara, T. Verkerk, S. Bliss, et al. 2021. The SPPL3-defined glycosphingolipid repertoire orchestrates HLA class I-mediated immune responses. [Published erratum appears in 2021 *Immunity* 54: 387.] *Immunity* 54: 132–150.e9.
- Dersh, D., J. D. Phelan, M. E. Gumina, B. Wang, J. H. Arbuckle, J. Holly, R. J. Kishon, T. E. Markowitz, M. O. Seedhom, N. Fridlyand, et al. 2021. Genome-wide screens identify lineage- and tumor-specific genes modulating MHC-I- and MHC-II-restricted immunosurveillance of human lymphomas. *Immunity* 54: 116–131.e10.
- Burr, M. L., C. E. Sparbier, K. L. Chan, Y. C. Chan, A. Kersbergen, E. Y. N. Lam, E. Azidis-Yates, D. Vassiliadis, C. C. Bell, O. Gilan, et al. 2019. An evolutionarily conserved function of polycomb silences the MHC class I antigen presentation pathway and enables immune evasion in cancer. *Cancer Cell* 36: 385–401.e8.
- Ennishi, D., K. Takata, W. Béguelin, G. Duns, A. Mottok, P. Farinha, A. Bashashati, S. Saberli, M. Boyle, B. Meissner, et al. 2019. Molecular and genetic characterization of MHC deficiency identifies EZH2 as therapeutic target for enhancing immune recognition. *Cancer Discov.* 9: 546–563.
- Sade-Feldman, M., Y. J. Jiao, J. H. Chen, M. S. Rooney, M. Barzilay-Rokni, J. P. Eliane, S. L. Bjorgaard, M. R. Hammond, H. Vitzthum, S. M. Blackmon, et al. 2017. Resistance to checkpoint blockade therapy through inactivation of antigen presentation. *Nat. Commun.* 8: 1136.
- Lazaridou, M. F., E. Gonschorek, C. Massa, M. Friedrich, D. Handke, A. Mueller, S. Jasinski-Bergner, R. Dummer, P. Koelblinger, and B. Seliger. 2020. Identification of miR-200a-5p targeting the peptide transporter TAP1 and its association with the clinical outcome of melanoma patients. *OncolImmunology* 9: 1774323.
- Lee, J. H., E. Shklovskaya, S. Y. Lim, M. S. Carlino, A. M. Menzies, A. Stewart, B. Pedersen, M. Irvine, S. Alavi, J. Y. H. Yang, et al. 2020. Transcriptional downregulation of MHC class I and melanoma de-differentiation in resistance to PD-1 inhibition. *Nat. Commun.* 11: 1897.
- Neeffjes, J. J., and H. L. Ploegh. 1988. Allele and locus-specific differences in cell surface expression and the association of HLA class I heavy chain with  $\beta_2$ -microglobulin: differential effects of inhibition of glycosylation on class I subunit association. *Eur. J. Immunol.* 18: 801–810.
- Stam, N. J., T. M. Vroom, P. J. Peters, E. B. Pastoors, and H. L. Ploegh. 1990. HLA-A- and HLA-B-specific monoclonal antibodies reactive with free heavy chains in Western blots, in formalin-fixed, paraffin-embedded tissue sections and in cryo-immuno-electron microscopy. *Int. Immunol.* 2: 113–125.
- Joung, J., S. Koenemann, J. S. Gootenberg, O. O. Abudayyeh, R. J. Platt, M. D. Brigham, N. E. Sanjana, and F. Zhang. 2017. Genome-scale CRISPR-Cas9 knockout and transcriptional activation screening. [Published erratum appears in 2019 *Nat. Protoc.* 14: 2259.] *Nat. Protoc.* 12: 828–863.
- Spahn, P. N., T. Bath, R. J. Weiss, J. Kim, J. D. Esko, N. E. Lewis, and O. Harismendy. 2017. PinAPL-Py: a comprehensive web-application for the analysis of CRISPR/Cas9 screens. *Sci. Rep.* 7: 15854.
- Schmidt, D., M. D. Wilson, C. Spyrou, G. D. Brown, J. Hadfield, and D. T. Odom. 2009. ChIP-seq: using high-throughput sequencing to discover protein-DNA interactions. *Methods* 48: 240–248.
- Amir, A. L., D. M. van der Steen, M. M. van Loenen, R. S. Hagedoorn, R. de Boer, M. D. Kester, A. H. de Ru, G. J. Lugthart, C. van Kooten, P. S. Hiemstra, et al. 2011. PRAME-specific allo-HLA-restricted T cells with potent antitumor reactivity useful for therapeutic T-cell receptor gene transfer. *Clin. Cancer Res.* 17: 5615–5625.
- van Amerongen, R. A., S. Tuit, A. K. Wouters, M. van de Meent, S. L. Siekman, M. H. Meeuwssen, T. L. A. Wachsmann, D. F. G. Remst, R. S. Hagedoorn, D. M.

- van der Steen, et al. 2023. PRAME and CTCFL-reactive TCRs for the treatment of ovarian cancer. *Front. Immunol.* 14: 1121973.
25. de Nappoles, M., J. E. Mermoud, R. Wakao, Y. A. Tang, M. Endoh, R. Appanah, T. B. Nesterova, J. Silva, A. P. Otte, M. Vidal, et al. 2004. Polycomb group proteins Ring1A/B link ubiquitylation of histone H2A to heritable gene silencing and X inactivation. *Dev. Cell* 7: 663–676.
  26. Fursova, N. A., N. P. Blackledge, M. Nakayama, S. Ito, Y. Koseki, A. M. Farcas, H. W. King, H. Koseki, and R. J. Klose. 2019. Synergy between variant PRC1 complexes defines polycomb-mediated gene repression. *Mol. Cell* 74: 1020–1036.e8.
  27. Scheuermann, J. C., A. G. de Ayala Alonso, K. Oktaba, N. Ly-Hartig, R. K. McGinty, S. Fraterman, M. Wilm, T. W. Muir, and J. Müller. 2010. Histone H2A deubiquitinase activity of the Polycomb repressive complex PR-DUB. *Nature* 465: 243–247.
  28. Scelfo, A., D. Fernández-Pérez, S. Tamburri, M. Zanotti, E. Lavarone, M. Soldi, T. Bonaldi, K. J. Ferrari, and D. Pasini. 2019. Functional landscape of PCGF proteins reveals both RING1A/B-dependent and RING1A/B-independent-specific activities. *Mol. Cell* 74: 1037–1052.e7.
  29. Blackledge, N. P., and R. J. Klose. 2021. The molecular principles of gene regulation by Polycomb repressive complexes. *Nat. Rev. Mol. Cell Biol.* 22: 815–833.
  30. Carbone, M., L. K. Ferris, F. Baumann, A. Napolitano, C. A. Lum, E. G. Flores, G. Gaudino, A. Powers, P. Bryant-Greenwood, T. Krausz, et al. 2012. BAP1 cancer syndrome: malignant mesothelioma, uveal and cutaneous melanoma, and MIB1. *J. Transl. Med.* 10: 179.
  31. Xie, J., L. Qiao, G. Deng, N. Liang, L. Xing, and J. Zhang. 2022. PCGF1 is a prognostic biomarker and correlates with tumor immunity in gliomas. *Ann. Transl. Med.* 10: 227.
  32. Ji, G., W. Zhou, J. Du, J. Zhou, D. Wu, M. Zhao, L. Yang, and A. Hao. 2021. PCGF1 promotes epigenetic activation of stemness markers and colorectal cancer stem cell enrichment. *Cell Death Dis.* 12: 633.
  33. Haworth, K. B., J. L. Leddon, C. Y. Chen, E. M. Horwitz, C. L. Mackall, and T. P. Cripe. 2015. Going back to class I: MHC and immunotherapies for childhood cancer. *Pediatr. Blood Cancer* 62: 571–576.
  34. Berghuis, D., A. S. de Hooge, S. J. Santos, D. Horst, E. J. Wiertz, M. C. van Eggermond, P. J. van den Elsen, A. H. Taminiau, L. Ottaviano, K. L. Schaefer, et al. 2009. Reduced human leukocyte antigen expression in advanced-stage Ewing sarcoma: implications for immune recognition. *J. Pathol.* 218: 222–231.
  35. Sugishita, H., T. Kondo, S. Ito, M. Nakayama, N. Yakushiji-Kaminatsui, E. Kawakami, Y. Koseki, Y. Ohinata, J. Sharif, M. Harachi, et al. 2021. Variant PCGF1-PRC1 links PRC2 recruitment with differentiation-associated transcriptional inactivation at target genes. *Nat. Commun.* 12: 5341.
  36. Blackledge, N. P., A. M. Farcas, T. Kondo, H. W. King, J. F. McGouran, L. L. P. Hanssen, S. Ito, S. Cooper, K. Kondo, Y. Koseki, et al. 2014. Variant PRC1 complex-dependent H2A ubiquitylation drives PRC2 recruitment and polycomb domain formation. *Cell* 157: 1445–1459.
  37. Kahn, T. G., E. Dorafshan, D. Schultheis, A. Zare, P. Stenberg, I. Reim, V. Pirrotta, and Y. B. Schwartz. 2016. Interdependence of PRC1 and PRC2 for recruitment to Polycomb response elements. *Nucleic Acids Res.* 44: 10132–10149.
  38. Figueiredo, C. R., H. Kalirai, J. J. Sacco, R. A. Azevedo, A. Duckworth, J. R. Slupsky, J. M. Coulson, and S. E. Coupland. 2020. Loss of BAP1 expression is associated with an immunosuppressive microenvironment in uveal melanoma, with implications for immunotherapy development. *J. Pathol.* 250: 420–439.
  39. Kaler, C. J., J. J. Dollar, A. M. Cruz, J. N. Kuznetsoff, M. I. Sanchez, C. L. Decatur, J. D. Licht, K. S. M. Smalley, Z. M. Correa, S. Kurtenbach, and J. W. Harbour. 2022. BAP1 loss promotes suppressive tumor immune microenvironment via upregulation of PROS1 in class 2 uveal melanomas. *Cancers (Basel)* 14: 3678.
  40. Zhang, C., and S. Wu. 2023. BAP1 mutations inhibit the NF- $\kappa$ B signaling pathway to induce an immunosuppressive microenvironment in uveal melanoma. *Mol. Med.* 29: 126.
  41. Blackledge, N. P., N. A. Fursova, J. R. Kelley, M. K. Huseyin, A. Feldmann, and R. J. Klose. 2020. PRC1 catalytic activity is central to polycomb system function. *Mol. Cell* 77: 857–874.e9.
  42. Zepeda-Martinez, J. A., C. Pribitzer, J. Wang, D. Bsteh, S. Golumbeanu, Q. Zhao, T. R. Burkard, B. Reichhoff, S. K. Rhie, J. Jude, et al. 2020. Parallel PRC2/cPRC1 and vPRC1 pathways silence lineage-specific genes and maintain self-renewal in mouse embryonic stem cells. *Sci. Adv.* 6: eaax5692.
  43. Cao, Q., X. Wang, M. Zhao, R. Yang, R. Malik, Y. Qiao, A. Poliakov, A. K. Yocum, Y. Li, W. Chen, et al. 2014. The central role of EED in the orchestration of polycomb group complexes. *Nat. Commun.* 5: 3127.
  44. He, M., M. S. Chaurushiya, J. D. Webster, S. Kummerfeld, R. Reja, S. Chaudhuri, Y. J. Chen, Z. Modrusan, B. Haley, D. L. Dugger, et al. 2019. Intrinsic apoptosis shapes the tumor spectrum linked to inactivation of the deubiquitinase BAP1. *Science* 364: 283–285.
  45. Fursova, N. A., A. H. Turberfield, N. P. Blackledge, E. L. Findlater, A. Lastuvkova, M. K. Huseyin, P. Dobrinic, and R. J. Klose. 2021. BAP1 constrains pervasive H2AK119ub1 to control the transcriptional potential of the genome. *Dev. Cell* 55: 749–770.
  46. He, M., M. S. Chaurushiya, J. D. Webster, S. Kummerfeld, R. Reja, S. Chaudhuri, Y. J. Chen, Z. Modrusan, B. Haley, D. L. Dugger, et al. 2019. Intrinsic apoptosis shapes the tumor spectrum linked to inactivation of the deubiquitinase BAP1. *Science* 364: 283–285.
  47. Luo, X., Y. Xu, Y. Li, G. Zhang, S. Huang, X. Liu, Z. Ren, S. Liu, and L. Yu. 2021. BAP1 deletion abrogates growth and metastasis of murine cutaneous melanoma. *Melanoma Res.* 31: 119–129.
  48. Koopmans, A. E., R. M. Verdijk, R. W. Brouwer, T. P. van den Bosch, M. M. van den Berg, J. Vaarwater, C. E. Kockx, D. Paridaens, N. C. Naus, M. Nellist, et al. 2014. Clinical significance of immunohistochemistry for detection of BAP1 mutations in uveal melanoma. *Mod. Pathol.* 27: 1321–1330.
  49. Perez-Garcia, V., G. Lea, P. Lopez-Jimenez, H. Okkenhaug, G. J. Burton, A. Moffett, M. Y. Turco, and M. Hemberger. 2021. BAP1/ASXL complex modulation regulates epithelial-mesenchymal transition during trophoblast differentiation and invasion. *eLife* 10: e63254.